Conformation of HIV-1 Envelope governs rhesus CD4 usage and simian-human immunodeficiency virus replication

Geraldine Vilmen[1], Anna C. Smith[1], Hector Cervera Benet[2], Rajni Kant Shukla[1], Ross C. Larue[3], Alon Herschhorn[2], Amit Sharma[1] *

[1]Department of Veterinary Biosciences, Department of Microbial Infection & Immunity, The Ohio State University, Columbus, OH.

[2]Division of Infectious Diseases and International Medicine, Department of Medicine, University of Minnesota, Minneapolis, MN.

[3]Department of Cancer Biology and Genetics, The Ohio State University, Columbus, OH.

*Address correspondence to:

Amit Sharma, PhD

Department of Veterinary Biosciences,

Department of Microbial Infection & Immunity,

The Ohio State University,

Columbus, OH 43210.

Email: sharma.157@osu.edu

Running title: Conformation of HIV Envelope governs rhesus CD4 usage.

Keywords: HIV-1 Envelope, CD4, Rhesus macaque, SHIV, Conformation, Viral entry.

Abstract

Infection of rhesus macaques with simian-human immunodeficiency viruses (SHIVs) is the preferred model system for vaccine development because SHIVs encode HIV-1 envelope glycoproteins (Env) – a key target of HIV-1 neutralizing antibodies. Since the goal of vaccines is to prevent new infections, SHIVs encoding circulating HIV-1 Env are desired as challenge viruses. Development of such biologically relevant SHIVs has been challenging as they fail to infect rhesus macaques, mainly because most circulating HIV-1 Env do not use rhesus CD4 (rhCD4) receptor for viral entry. Most primary HIV-1 Env exist in a closed conformation and occasionally transit to downstream, open conformation through an obligate intermediate conformation. Here, we provide genetic evidence that open Env conformations can overcome the rhCD4 entry barrier and increase replication of SHIVs in rhesus lymphocytes. Consistent with prior studies, we found that circulating HIV-1 Env do not use rhCD4 efficiently for viral entry. However, using HIV-1 Env with single amino acid substitutions that alter their conformational state, we found that transitions to intermediate and open Env conformation allow usage of physiological levels of rhCD4 for viral entry. We engineered these single amino acid substitutions in the transmitted/founder HIV-1_{BG505} Env encoded by SHIV-BG505 and found that open Env conformation enhances SHIV replication in rhesus lymphocytes. Lastly, CD4-mediated SHIV pull-down, sensitivity to soluble CD4, and fusogenicity assays indicated that open Env conformation promotes efficient rhCD4 binding and viral-host membrane fusion. These findings identify conformational state of HIV-1 Env as a major determinant for rhCD4 usage, viral fusion, and SHIV replication.

55 **Importance**

56 Rhesus macaques are critical animal model for preclinical testing of HIV-1 vaccine and prevention
57 approaches. However, HIV-1 does not replicate in rhesus macaques, and thus chimeric simian-
58 human immunodeficiency viruses (SHIVs), which encode HIV-1 envelope glycoproteins, are used
59 as surrogate challenge viruses to infect rhesus macaques for modeling HIV-1 infection.
60 Development of SHIVs encoding envelope from clinically relevant, circulating HIV-1 variants has
61 been extremely challenging as such SHIVs replicate poorly, if at all, in rhesus lymphocytes. This
62 is because most circulating HIV-1 envelope do not use rhesus CD4 efficiently for viral entry. In
63 this study, we identify conformational state of HIV-1 envelope as a key determinant for rhesus
64 CD4 usage, viral-host membrane fusion, and SHIV replication in rhesus lymphocytes.

65

66

67

68

69

70

71

72

73

74

75

76

77 **Introduction**

78 The ability of viruses to efficiently utilize orthologous entry receptors determines which species
79 can be infected, and this principle is often exploited for developing animal models of viral infection.
80 Rhesus macaques serve as critical animal model for pre-clinical HIV-1 research. However,
81 macaque models are limited by the fact that HIV-1 does not persistently infect macaques.
82 Chimeric simian-human immunodeficiency viruses (SHIVs), constructed by replacing SIV
83 envelope glycoproteins (Env) with that from HIV-1, have been developed as surrogates to study
84 HIV-1 infection in rhesus macaques (1). Development of SHIVs has been a challenging process,
85 mainly because most Env from circulating HIV-1 variants do not use rhesus CD4 (rhCD4)
86 efficiently for viral entry, and, therefore, SHIVs replicate poorly in rhesus lymphocytes and do not
87 establish persistent infection (2). Existing pathogenic SHIVs are a highly selected subset of
88 viruses because they encode Env from lab-adapted and chronic-stage HIV-1 variants, which can
89 mediate entry using rhCD4. Moreover, to increase their pathogenicity SHIVs generally require
90 extensive adaptation to macaques (3-8), at least in part to optimize rhCD4-mediated entry (9).
91 However, adaptation alters the antigenic features of Env (10), limiting the translational utility of
92 adapted SHIVs.

93 Binding of the metastable HIV-1 Env trimer to CD4 triggers a series of conformational changes in
94 Env i.e., the Env transitions from a functionally 'closed' (state 1) to an 'intermediate' (state 2) to
95 an 'open' (state 3) conformation (11-13). Unliganded Env trimer of primary isolates only
96 infrequently transit from closed to downstream, more open states (11, 14). The conformational
97 dynamics of HIV-1 Env can affect viral tropism by allowing adaptability to cells with different CD4
98 levels. For example, HIV-1 Env that frequently sample state 2 and state 3 conformations can more
99 efficiently infect cells that express low levels of human CD4 (huCD4) (15, 16). Importantly, the
100 ability of HIV-1 Env to utilize low levels of huCD4 positively correlates with their ability to utilize
101 rhCD4 (17). Based on these insights, we hypothesized that open conformational states of HIV-1

102 Env can overcome the rhCD4 entry barrier, which can in turn increase replication of SHIVs in
103 rhesus lymphocytes. In this study, we generated HIV-1 Env and SHIVs with single amino acid
104 substitutions that alter the conformational state of Env. Our results show that SHIVs with open
105 Env conformation bind and utilize rhCD4 efficiently and display higher viral fusion and replication
106 in rhesus lymphocytes.

107 **Results**

108 **Transmitted/founder and early-stage HIV-1 Envs do not use physiological levels of rhCD4**
109 **efficiently for viral entry.**

110 Env from most circulating HIV-1 isolates from early stages of infection, including the
111 transmitted/founder (T/F) variants, do not use rhCD4 efficiently for viral entry (17). To test our
112 hypothesis, that open Env conformations can overcome the rhCD4 entry barrier and mediate entry
113 using physiological levels of rhCD4 expressed on rhesus lymphocytes, we first generated
114 Cf2Th/syn CCR5 cells that stably express either low or high levels of rhCD4 ($rhCD4_{LOW}$,
115 $rhCD4_{HIGH}$). Importantly, we sorted and selected the $rhCD4_{LOW}$ cells such that their CD4
116 expression levels is representative of primary rhesus lymphocytes (**Figure 1**). The cells were then
117 infected with GFP-reporter HIV-1 pseudotyped with Env that were obtained from HIV-1 isolates
118 from acute/early stages of infection, including the T/F isolates (**Table 1**). As control, Cf2Th/syn
119 CCR5 cells expressing huCD4 were also infected and facilitated entry by all of these Env (**Figure**
120 **2**). In contrast to huCD4-mediated entry, $rhCD4_{LOW}$ cells did not facilitate efficient entry by seven
121 out of eight Env. Even with $rhCD4_{HIGH}$ cells, which express high levels of rhCD4, viral entry was
122 much lower (~2.5–53-fold) than the huCD4. Only subtype D Env 191859 was able to gain entry
123 in $rhCD4_{LOW}$ cells but it was still ~1.7-fold lower than huCD4, highlighting that there are some rare
124 primary Env that can inherently utilize rhCD4. As positive controls, two Env from chronic-stage
125 HIV-1 isolates (JR-FL and BaL) were able to gain entry using both huCD4 and rhCD4 – consistent
126 with the ability of Env from lab-adapted and chronic-stage isolates to utilize rhCD4 for entry (17).

127 **Transitions to intermediate and open Env conformations allow usage of rhCD4 for viral**
128 **entry.**

129 Recent studies have suggested that Env of most primary HIV-1 isolates exist in a closed
130 conformation and only infrequently transit to downstream, more open conformations (11, 13, 18,
131 19). The ability of unliganded or CD4-bound Env to transit to downstream states can affect viral
132 tropism by allowing adaptability to cells with different CD4 levels (15, 16). Thus, we sought to
133 determine how the conformational states of HIV-1 Env affects its ability to utilize rhCD4 for viral
134 entry. We took advantage of the fact that single amino acid substitutions in the gp120 domain of
135 Env can alter its conformational state (15, 16). For example, L193A substitution in the V1/V2 loop
136 of gp120 allows Env to populate the state 2 conformation. I423A substitution in the β20-β21
137 element of gp120 allows Env to populate the state 3 conformation. We engineered L193A and
138 I423A substitutions in three different Env representing a T/F (BG505.W6M.C2), an acute stage
139 (ZM53M.PB12), and a chronic stage (JR-FL) isolate. For the two early-stage Env, I423A
140 substitution mediated entry in $rhCD4_{LOW}$, $rhCD4_{HIGH}$, and huCD4 cells with similar efficiency,
141 whereas the L193A substitution displayed lower efficiency of entry in $rhCD4_{LOW}$ cells when
142 compared to huCD4 and $rhCD4_{HIGH}$ (**Figure 3A and 3B**). As control, the related wild type (WT)
143 Env utilized huCD4 efficiently but did not gain efficient entry even in cells that express high levels
144 of rhCD4. The chronic-stage JR-FL Env was able to gain entry using both huCD4 and rhCD4 –
145 independent of Env conformational state or rhCD4 expression levels (**Figure 3C**). Similar patterns
146 of rhCD4 usage were observed at different multiplicities of infection indicating that the ability of
147 open Env conformations to use physiological levels of rhCD4 is independent of virus input (**Figure**
148 **S1**). Thus, our results suggest that single amino acid substitutions in Env that promote transitions
149 to intermediate and open conformations allow usage of physiological levels of rhCD4 for viral
150 entry.

151 **Open Env conformations promote replication of SHIV-BG505 in rhesus lymphocytes.**

152 Next, we sought to determine whether improved rhCD4 usage by Env that are in intermediate and
153 open conformational states translate into enhanced replication of T/F SHIV in rhesus
154 lymphocytes. For this purpose, we introduced the L193A or I423A substitution in the HIV-1_{BG505}
155 T/F Env encoded by SHIV-BG505. Importantly, we also included SHIV-BG505 with A204E
156 substitution in the C1 region of gp120 as a benchmark control for replication. The A204E adaptive
157 mutation, previously identified through serial passage of primary HIV-1 Env in immortalized
158 macaque $CD4^+$ T-lymphocytes (20), was sufficient to mediate viral entry in $rhCD4_{LOW}$ cells at
159 levels comparable to huCD4 (**Figure S2**). More importantly, the A204E substitution induces
160 conformational changes in the Env that opens up the Env trimers on the surface of virions (10),
161 which likely explains its ability to utilize physiological levels of rhCD4. We measured the ability of
162 these SHIVs to replicate in the immortalized rhesus macaque $CD4^+$ T- lymphocytes (21). As
163 expected, the replication of SHIV encoding wild-type Env (WT SHIV), which does not utilize rhCD4
164 efficiently, declined over the 15-day time course indicating that it does not replicate in rhesus cells
165 (**Figure 4A and 4B**). SHIVs encoding I423A or A204E substitutions replicated to significantly
166 higher levels over the 15-day time course when compared to WT SHIV. Interestingly, SHIV
167 L193A, which encodes Env with an intermediate open conformation that allows it to use rhCD4
168 better than the WT Env (**Figure 3A**), did not display significantly improved growth kinetics when
169 compared to WT SHIV. Based on these findings, we conclude that open Env conformations, such
170 as those conferred by I423A and A204E mutations, promote replication of SHIV-BG505 in rhesus
171 lymphocytes.

172 **Open Env conformations promote CD4 binding and viral fusion.**

173 Finally, we examined whether open Env conformations promote SHIV replication by enhancing
174 rhCD4 binding and viral fusion. We evaluated the effects of Env conformation on rhCD4 binding
175 by two independent approaches. First, we performed neutralization assays to measure the ability
176 of soluble rhCD4 to bind functional Env trimers on SHIVs and compete with receptor binding to

177 inhibit viral entry. WT SHIV was least sensitive to rhCD4 inhibition indicating that it does not
178 efficiently bind rhCD4 and interfere with receptor binding (**Figure 5A**). SHIV L193A and SHIV
179 I423A, which are stabilized in State 2 and State 3 Env conformation, respectively, were ~3-fold
180 and ~30-fold more sensitive to rhCD4 inhibition when compared to WT SHIV, suggesting that
181 progressive opening of the Env increases rhCD4 binding. SHIV A204E was most sensitive
182 (~1500-fold) to rhCD4 inhibition suggesting that it has the highest binding for rhCD4, likely
183 attributable to 'more open' conformation of its Env trimers. Similar neutralization trends, but with
184 ~2−10-fold more potent inhibition, were observed with soluble huCD4 indicating that HIV-1 Env
185 encoded by these SHIVs bind huCD4 with higher affinity than rhCD4 (**Figure S3A**). Second, we
186 employed a qualitative affinity pull-down assay to determine the binding of rhCD4 to Env
187 expressed on infectious SHIVs. Virions bound to His-tagged rhCD4 were affinity precipitated and
188 their Env levels were measured by immunoblotting. Consistent with the results of the
189 neutralization assay, progressive opening of the Env resulted in more virions binding to rhCD4;
190 with highest binding observed in case of SHIV A204E (**Figure 5B**). Similar binding patterns were
191 also observed when pull-downs were performed with huCD4 (**Figure S3B**). Lastly, we
192 investigated how Env conformation affects fusion of SHIVs with rhesus lymphocytes using a SHIV
193 fusion assay. WT SHIVs, which did not efficiently bind rhCD4, were not fusogenic with the target
194 cells (**Figure 5C and 5D**). SHIV L193A and SHIV I423A, which are stabilized in State 2 and State
195 3 Env conformation, respectively, were ~7-fold and ~25-fold more fusogenic when compared to
196 WT SHIV, suggesting that fusogenicity increases with progressive opening of the Env. SHIV
197 A204E was the most fusogenic with ~87-fold higher fusion than WT SHIV. Taken together, our
198 results demonstrate that open Env conformations, such as those conferred by I423A and A204E
199 mutations, increase binding of Env to rhCD4 and subsequent SHIV-host membrane fusion.

200

201

202 **Discussion**

203 Here, we provide first genetic evidence that conformational state of HIV-1 Env governs rhCD4
204 usage. Using HIV-1 Env with single amino acid substitutions that alter their conformational state,
205 we demonstrated that transitions to intermediate and open Env conformations allow usage of
206 physiological levels of rhCD4 for viral entry, which is otherwise a suboptimal receptor for entry.
207 Moreover, by introducing these changes in isogenic SHIV backbone, we found that open Env
208 conformations promote rhCD4 binding, fusion-mediated cell entry, and replication in rhesus
209 lymphocytes.

210 Thermodynamically, most primary HIV-1 Env are in a high free energy, closed conformation.
211 Single-molecule fluorescence resonance energy transfer studies have demonstrated that either
212 spontaneously or upon CD4 binding, Env transitions from closed (state 1) to open conformation
213 (state 3) through a functional intermediate (state 2) (11). Multiple amino acid residues restrain
214 Env in state 1 and CD4 binding triggers Env transitions from state 1 to downstream, lower-energy
215 states (15, 16, 22-25). For example, L193A and I423A substitution releases the state 1 restraints
216 and stabilizes Env in State 2 and State 3 conformation, respectively. Our findings of improved
217 rhCD4 usage by Envs bearing L193A and I423A substitutions suggest that transitions to
218 intermediate and open conformations advance HIV-1 Env on the entry pathway and likely facilitate
219 Env engagement with a suboptimal rhCD4 receptor. Although Env with L193A substitutions, which
220 are in intermediate open conformation, utilized rhCD4 better than WT Env, SHIV encoding L193A
221 substitution did not display significantly improved viral fusion and replication. In contrast, SHIVs
222 encoding Env with I423A and A204E substitutions, which are in open conformation, displayed
223 significantly increased rhCD4 engagement, viral fusion, and replication. These results indicate
224 that open Env conformations, such as those conferred by I423A and A204E mutations, promote
225 rhCD4 binding, viral fusion, and replication of SHIV in rhesus lymphocytes. Collectively, these
226 findings suggest that modulating the conformational dynamics of viral Env by altering select amino

227 acid residues can help overcome the cross-species entry barrier, which in turn facilitates
228 replication and adaptation of the virus in a new host species.

229 While our findings suggest that downstream, open Env conformations allow usage of rhCD4, it
230 also highlights that most T/F and early-stage HIV-1 Envs likely have an inherently low propensity
231 to sample downstream, open conformations. For instance, only one of the eight early-stage Env
232 tested was able to use physiological levels of rhCD4 for viral entry. This explains why development
233 of SHIVs encoding T/F and early-stage Envs has been challenging and often require extensive
234 adaptation in human and/or rhesus lymphocytes – process that selects for open Env conformation
235 (2, 10, 20). Consistent with this notion, SHIV-BG505 encoding A204E adaptive mutation,
236 previously identified through *in vitro* evolution experiments (20), displayed highest replication in
237 rhesus lymphocytes; viral-host membrane fusion; and sensitivity to soluble CD4. These findings
238 also offer an explanation as to why some existing pathogenic SHIVs derived using primary HIV-
239 1 Envs display high sensitivity to soluble CD4 (26-28) – a proxy measure for open Env
240 conformation where the CD4 binding site is exposed.

241 In summary, our findings have helped identify a key parameter for future design of SHIVs –
242 conformational state of Env. Considerable efforts are being made to engineer SHIVs that encode
243 circulating HIV-1 Env; utilize rhCD4 for entry; replicate in rhesus macaques without extensive
244 adaptation; and retain as much of the biological characteristics of HIV-1 Env as possible (29-31).
245 Thus, it will be of interest to identify and define the minimal open conformational state of HIV-1
246 Env that affords usage of rhCD4 and replication of SHIVs in rhesus macaques with minimal impact
247 on Env trimer structure and antigenic profile. Based on the findings of this study, the following
248 considerations could be useful for SHIV design: 1) selection of circulating HIV-1 Env with high
249 inherent propensity to sample downstream, open conformations; and 2) engineering changes in
250 Env that lower free energy needed for transition to open conformations without significantly
251 altering its antigenicity.

252 **Materials and Methods**

253 **Cells, envelope clones, plasmids, proteins**

254 HEK293T (ATCC CRL-3216), HeLa TZM-bl (32) (NIH AIDS Reagent program catalog no. 8129),
255 and Cf2Th/syn CCR5 (33) (NIH AIDS Reagent program catalog no. 4662) cells were cultured in
256 Dulbecco's modified eagle medium (DMEM, Gibco) supplemented with 10% fetal bovine serum
257 (FBS, Sigma), 2 mM L-glutamine (Gibco), and 1x Penicillin-Streptomycin (Gibco) (complete
258 DMEM). Cf2Th/syn CCR5, which are engineered to express human CCR5, were further
259 supplemented with 400 µg/ml of Geneticin (Gibco) to maintain CCR5 expression. Immortalized
260 rhesus macaque 221 T-lymphocytes (21) were cultured in Iscove's modified Dulbecco's medium
261 (IMDM) supplemented with 10% FBS, 2 mM L-glutamine, and 1x Penicillin-Streptomycin, and 100
262 U/ml of interleukin-2 (Roche) (complete IMDM). Rhesus macaque peripheral blood mononuclear
263 cells (PBMCs) were isolated from whole blood (Washington National Primate Research Center)
264 from two independent donors using human erythrocyte lysing kit (R&D Systems) and 95%
265 Lymphoprep (Stemcell Technologies) following manufacturer's protocols.

266 The following Env clones from early HIV-1 infections were used: BG505.W6M.C2; Q23.17;
267 TRO.11; CAAN5342.A2; Du422.1; ZM53M.PB12; QB857.110I.B3; and 191859. As control, two
268 Env clones (JR-FL and BaL.01) of chronic HIV-1 strains were used. The following Env clones
269 encoding the L193A, I423A or A204E mutations were used: BG505.W6M.C2; ZM53M.PB12; and
270 JR-FL.

271 β-lactamase (BlaM) gene fused to the N-terminus of SIVmac239 Vpr (Genbank: M33262)
272 separated by six-glycine-one-lysine linker was synthesized as a DNA fragment (Integrated DNA
273 Technologies), digested, and ligated into pcDNA3.1 (Invitrogen) using KpnI and NotI restriction
274 sites to generate pcDNA3.1-Blam-SIVmac239 Vpr plasmid. All plasmids generated in this study
275 were verified by Sanger DNA sequencing.

276 Soluble rhCD4 (Met1-Trp390; catalog no. 90274-C08H) and huCD4 (Met 1-Trp 390; catalog no.
277 10400-H08H) proteins with C-terminus 6x-His-tags were purchased from Sino Biological.

278 **Pseudovirus and SHIV production**

279 Green fluorescent protein (GFP) reporter pseudoviruses were generated as described previously
280 (34). Briefly, HEK293T cells were cotransfected with 4 µg of Env-deficient HIV-1 proviral plasmid
281 (Q23ΔEnvGFP) and 2 µg of HIV-1 Env clone of interest using Fugene 6 transfection reagent
282 (Roche) following manufacturer's protocol. Replication-competent SHIV stocks were generated
283 as described previously (35). The viral titer of each pseudovirus and SHIV stock was determined
284 by infecting TZM-bl cells and staining for β-galactosidase activity 48 hours post-infection (32).

285 **Generation of stable cell lines**

286 Cf2Th/syn CCR5 cells stably expressing rhCD4 were generated using methods described
287 previously (36). Briefly, retroviral pseudoviruses were generated in HEK293T cells by
288 cotransfecting pLPCX-rhCD4 (retroviral vector encoding rhCD4), pJK3 (MLV-based packaging
289 plasmid), and pMD.G (vesicular stomatitis virus glycoprotein [VSV-G] plasmid) at a ratio of 1:1:0.5
290 using Fugene 6 transfection reagent following manufacturer's protocol. Forty-eight hours post-
291 transfection, the pseudoviruses were concentrated and used to transduce 10^5 Cf2Th/syn CCR5
292 cells. Transduced cells were cultured in complete DMEM supplemented with 400 µg/ml of
293 Geneticin (to maintain CCR5 expression) and 2 µg/ml of puromycin (to select for CD4 expression,
294 Sigma). The drug selected cells with low ($rhCD4_{LOW}$) or high ($rhCD4_{HIGH}$) levels of rhCD4
295 expression were obtained by sorting the cells on a FACSAria II cell sorter (BD Biosciences) using
296 an allophycocyanin (APC)-conjugated CD4 monoclonal antibody (BD Biosciences catalog no.
297 551980) using previously described CD4 staining method (17). The $rhCD4_{LOW}$ cells were sorted
298 by gating on the CD4-expressing cell population that overlapped with the CD4-stained rhesus
299 macaque PBMCs. The $rhCD4_{HIGH}$ cells were sorted by gating on the top 20% of CD4-expressing

300 cell population. Cf2Th/syn CCR5 cells stably expressing huCD4 have been described previously
301 (36).

302 **CD4 infectivity assay**

303 Infection of Cf2Th/syn CCR5 cells expressing huCD4, rhCD4$_{LOW}$, and rhCD4$_{HIGH}$ with GFP
304 reporter pseudoviruses was performed as described previously (36). Briefly, cells were infected
305 at a multiplicity of infection (MOI) of 0.1, 0.25, and 1 in the presence of 10 µg/ml of DEAE-dextran
306 by spinoculation at 1200 x g for 90 minutes. After 48 hours, cells were harvested, fixed in 2%
307 paraformaldehyde, washed twice, and resuspended in fluorescence-activated cell sorter (FACS)
308 buffer (1x phosphate-buffered saline (PBS), 1% FBS, 1 mM EDTA). Cells were analyzed for GFP
309 expression on Attune NxT flow cytometer (Life Technologies). The data from ~10^4 cells were
310 analyzed using FlowJo version 10.7.1.

311 **Construction of SHIV proviral clones**

312 Full-length proviral SHIV plasmid encoding BG505.W6M.B1 Env (37) with A204E mutation (SHIV-
313 BG505 A204E) has been described previously (38). EcoRV-MfeI region of BG505.W6M.B1 Env
314 (wild type, WT) and its L193A and I423A variants were synthesized as DNA fragments (Twist
315 Biosciences). SHIV-BG505 WT, SHIV-BG505 L193A, and SHIV-BGB505 I423A proviral clones
316 were generated by digesting and ligating the DNA fragments into the SHIV-BG505 A204E proviral
317 plasmid using EcoRV and MfeI restriction sites. The generated SHIV proviral plasmids were
318 verified by DNA sequencing.

319 **SHIV replication time course**

320 Replication of SHIVs was assessed as described previously (35). Briefly, 4x10^6 221 T-
321 lymphocytes were infected at a MOI of 0.02 by spinoculation at 1200 x g for 90 minutes at room
322 temperature. After spinoculation, cells were washed four times with 1 ml of complete IMDM, re-
323 suspended in 5 ml of complete IMDM and plated in one well of a 6-well plate. Every three days,

324 two-third of the cultures were harvested and replenished with fresh, complete IMDM. Viral
325 supernatants were collected from the harvested cultures by pelleting at 650 x g for 5 minutes at
326 room temperature. RT activity in viral supernatants was measured using the RT activity assay.

327 **SHIV neutralization assay**

328 Neutralization of SHIVs with rhCD4 and huCD4 were performed as described previously (16) but
329 using TZM-bl target cells. The calculated half-maximal inhibitory concentration (IC_{50}) values
330 represent the soluble CD4 concentration in μM at which 50% of the virus was neutralized.

331 **CD4–SHIV binding assay**

332 Affinity pull-down assays were performed using Ni Sepharose 6 Fast Flow resin (Cytiva
333 Lifesciences); His-tagged rhCD4 or huCD4; and SHIV stocks to assess binding of CD4 to SHIVs.
334 20 μl of Ni-resin was equilibrated in binding buffer (50 mM HEPES pH 7.5, 250 mM NaCl, 50 mM
335 imidazole, and 2 mM β-mercaptoethanol) by washing three times (10,000 x g for 1 minute) with
336 100 μl of binding buffer. Equilibrated Ni-resin was incubated for 10 minutes with 1 μg of His-CD4
337 in 20 μl of binding buffer. Binding reactions were setup by adding equal amounts of indicated
338 SHIV virions (equivalent to 800 and 400 mU of RT) in 160 μl of binding buffer and incubated for
339 1 hour at room temperature, under rotation. Reactions were then washed three times (10,000 x g
340 for 1 minute) with 100 μl of binding buffer to remove unbound CD4/virions. The resulting CD4–
341 virion complexes bound to the Ni-resin were extracted using 4x Laemmli sample buffer (BioRad),
342 heated at 95°C for 5 minutes, and subjected to SDS-PAGE/Western blotting analysis. Standard
343 Western blotting procedures were used with the following antibodies: HIV-1 gp120 (NIH AIDS
344 Reagent program catalog no. 288) and 6x-His Tag (ThermoFisher catalog no. MA1-21315-HRP).

345 **SHIV fusion assay**

346 The HIV-1 β-lactamase-Vpr (BlaM-Vpr) virus fusion assay described previously (39, 40) was
347 modified to evaluate SHIV fusion. Briefly, BlaM-Vpr was modified by swapping the HIV-1 Vpr with

348 SIVmac239 Vpr to retain the cognate Gag p6-SIVmac Vpr interaction necessary for efficient virion
349 incorporation of Vpr (41). SHIVs containing Blam-SIVmac239 Vpr fusion protein were generated
350 by co-transfecting HEK293T cells with 4.5 µg of proviral SHIV plasmid and 1.5 µg of pcDNA3.1-
351 Blam-SIVmac239 Vpr plasmid using Fugene 6 transfection reagent following manufacturer's
352 protocol. Forty-eight hours post-transfection, virus-containing supernatant was harvested, passed
353 through a 0.2 µm sterile filter, concentrated ~10-fold using Amicon Ultracel 100 kDa filters
354 (Millipore), aliquoted and stored at -80°C. RT activity of viral stocks was measured using the RT
355 activity assay. 10^5 221 T-lymphocytes in 100 µl of complete IMDM were infected with Blam-
356 SIVmac239 Vpr-containing SHIVs equivalent to 720 mU of RT by spinoculation at 1200 x g for 90
357 minutes followed by incubation at 37°C and 5% CO_2 for one hour. Fusion-mediated SHIV entry
358 was quantified by monitoring the conversion of fluorescent BlaM CCF2-AM substrate dye as
359 described. After infection, cells were washed once with 300 µl of cold CO_2-independent media
360 (Gibco) without FBS and resuspended in 100 µl of CO_2-independent media supplemented with
361 10% FBS. Cells were incubated with CCF2-AM substrate (LiveBLAzer CCF2-AM Kit, Invitrogen)
362 following manufacturer's protocol in the presence of 1.8 mM Probenecid (Sigma) for 2 hours. Cells
363 were washed three times with 300 µl of cold CO_2-independent media without FBS, once with 1x
364 PBS, fixed with 200 µl of 2% paraformaldehyde, washed once with 1x PBS, and resuspended in
365 400 µl of FACS buffer. The fluorescence of cleaved CCF2-AM substrate was measured on Attune
366 NxT flow cytometer and data were analyzed using FlowJo version 10.7.1.

367 **Reverse transcriptase activity assay**

368 RT activity assay was performed as described previously (40, 42) with minor modifications.
369 Briefly, 5 µl of viral supernatant, viral stock or RT standard was lysed in 5 µl of 2x lysis buffer (100
370 mM Tris HCl pH 7.4, 50 mM KCl, 0.25% Triton X-100, 40% glycerol) in the presence of 4U
371 RNaseOUT (Invitrogen) for 10 minutes at room temperature. Viral lysate was diluted 1:10 by
372 adding 90 µl of nuclease-free water (Life Technologies). qRT-PCR reactions were prepared by

373 mixing 9.6 µl of diluted viral lysate with 10.4 µl of reaction mix containing 10 µl of 2x Maxima
374 SYBR Green/ROX qPCR Master Mix (ThermoFisher), 0.1 µl of 4U/µl RNaseOUT, 0.1 µl of 0.8
375 µg/µl MS2 RNA template (Roche), and 0.1 µl each of 100 µM forward 5'-
376 TCCTGCTCAACTTCCTGTCGAG-3' and reverse 5'-CACAGGTCAAACCTCCTAGGAATG-3'
377 primers. qRT-PCR was performed using a QuantStudio 3 Real-Time PCR machine (Applied
378 Biosystems). Viral titers were calculated from a standard curve generated using recombinant
379 reverse transcriptase (Millipore catalog no. 382129).

380 **Figure Legends**

381 **Figure 1. Expression levels of rhCD4 stably introduced into Cf2Th/syn CCR5 cells.**
382 Expression levels of CD4s on primary rhesus macaque lymphocytes, and $rhCD4_{LOW}$ and
383 $rhCD4_{HIGH}$ Cf2Th/syn CCR5 cell lines as measured by flow cytometry using an APC-conjugated
384 anti-CD4 antibody. The histograms represent the expression of CD4 on the cell surface. The data
385 are representative of two independent experiments.

386 **Figure 2. Ability of transmitted/founder and early-stage HIV-1 Env to use physiological**
387 **levels of rhCD4 for viral entry.** Cf2Th/syn CCR5 cells expressing human or rhesus CD4
388 (indicated along the x-axis) were infected with HIV-$1_{Q23\Delta EnvGFP}$ pseudotyped with indicated Env
389 clones. Infection was measured by flow cytometry as percentage of GFP-positive cells 48 h post-
390 infection. Graphs indicate percentage of infected cells for indicated Env at multiplicity of infection
391 of 1. Env clones are labeled at the top, with first letter indicating the subtype. Bars represent the
392 average of three independent experiments. Error bars represent standard deviations.

393 **Figure 3. Effect of Env conformation on usage of rhCD4 for viral entry.** Cf2Th/syn CCR5
394 cells expressing human or rhesus CD4 (indicated along the x-axis) were infected with HIV-
395 $1_{Q23\Delta EnvGFP}$ pseudotyped with **(A)** BG505.W6M.C2, **(B)** ZM53M.PB12, and **(C)** JR-FL Env clone.
396 Infection was measured by flow cytometry as percentage of GFP-positive cells 48 h post-infection.

397 Graphs indicate percentage of infected cells for wild-type ('WT'), L193A, and I423A Env variants
398 at multiplicity of infection of 1. Bars represent the average of three independent experiments. Error
399 bars represent standard deviations.

400 **Figure 4. Effect of Env conformation on SHIV replication. (A)** Replication kinetics of SHIV-
401 BG505 variants in rhesus macaque 221 T-lymphocytes over a 15-day time course. Reverse
402 transcriptase (RT) activity in viral supernatants is plotted vs. days post-infection. The key at the
403 right of the graph indicates the identity of Env variant (wild-type 'WT' or indicated amino acid
404 mutation) encoded by each SHIV. Each data point represents the average of three independent
405 experiments, performed in duplicate. Error bars represent standard deviations. **(B)** Area under
406 the curve (AUC) for indicated SHIV variants (x-axis) determined from the replication curves shown
407 in (A). AUC values were compared to SHIV-BG505 WT using one-way analysis of variance
408 (ANOVA) followed by Dunnett's multiple comparisons test. *** p = 0.0004; ** p = 0.004; ns, not
409 significant.

410 **Figure 5. Effect of Env conformation on rhCD4 binding and viral fusion. (A)** Sensitivity of
411 SHIV-BG505 to neutralization by soluble rhCD4. Neutralization curves of the indicated SHIV
412 variants were generated by plotting percent residual infection (y-axis) against rhCD4
413 concentration (μM, x-axis). Each data point represents the average of two independent
414 experiments, performed in duplicate. Error bars represent standard deviations. The calculated
415 IC_{50}s are shown. Where IC_{50} values were above the highest tested concentration, the extrapolated
416 concentration is indicated by ‡. **(B)** Binding of SHIV-BG505 to rhCD4. Western blot analysis for
417 affinity pull-down of His-tagged rhCD4 with increasing amounts (400 and 800 mU of RT) of
418 indicated SHIV virions. Immunoblotting performed using anti-HIV-1 gp120 and anti-6x-His
419 antibodies. **(C)** Representative flow cytometry plots indicating percent viral fusion. Fusion of
420 indicated SHIV-BG505 with rhesus macaque 221 T-lymphocytes was measured as percentage
421 of cells with cleaved CCF-AM substrate. The identity of Env variant (wild-type 'WT' or indicated

422 amino acid mutation) encoded by each SHIV is indicated above the plots. **(D)** Graph indicate
423 percent viral fusion for indicated SHIV variants (x-axis). Data represents the average of three
424 independent experiments with individual data points shown as circles. Error bars represent
425 standard deviations. Percent viral fusion were compared to SHIV-BG505 WT using one-way
426 analysis of variance (ANOVA) followed by Dunnett's multiple comparisons test. **** $p < 0.0001$;
427 ** $p = 0.0024$; ns, not significant.

428 **Figure S1. Effect of virus input on rhCD4 usage by HIV-1 Envs in different conformations.**
429 Cf2Th/syn CCR5 cells expressing human or rhesus CD4 (indicated along the x-axis) were
430 infected with HIV-$1_{Q23\Delta EnvGFP}$ pseudotyped with **(A)** BG505.W6M.C2, **(B)** ZM53M.PB12, or **(C)** JR-
431 FL Env clone. Infection was measured by flow cytometry as percentage of GFP-positive cells 48
432 h post-infection. Graphs indicate percentage of infected cells for wild-type ('WT'), L193A, and
433 I423A Env variants at different multiplicity of infection ('MOI', *top panel* MOI 0.1, *bottom panel*
434 MOI 0.25). Bars represent the average of three independent experiments. Error bars represent
435 standard deviations.

436 **Figure S2. Ability of HIV-1 Env with A204E substitution to use physiological levels of rhCD4**
437 **for viral entry.** Cf2Th/syn CCR5 cells expressing human or rhesus CD4 (indicated along the x-
438 axis) were infected with HIV-$1_{Q23\Delta EnvGFP}$ pseudotyped with BG505 Env encoding A204E mutation.
439 Infection was measured by flow cytometry as percentage of GFP-positive cells 48 h post-infection.
440 Graphs indicate percentage of infected cells at indicated multiplicity of infection ('MOI'). Bars
441 represent the average of three independent experiments. Error bars represent standard
442 deviations.

443 **Figure S3. Effect of Env conformation on huCD4 binding. (A)** Sensitivity of SHIV-BG505 to
444 neutralization by soluble huCD4. Neutralization curves of the indicated SHIV variants were
445 generated by plotting percent residual infection (y-axis) against huCD4 concentration (μM, x-axis).
446 The key at the right of the graph indicates the identity of Env variant (wild-type 'WT' or indicated

447 amino acid mutation) encoded by each SHIV. Each data point represents the average of two
448 independent experiments, performed in duplicate. Error bars represent standard deviations. The
449 calculated IC_{50}s are shown. Where IC_{50} values were above the highest tested concentration, the
450 extrapolated concentration is indicated by ‡. **(B)** Binding of SHIV-BG505 to huCD4. Western blot
451 analysis for affinity pull-down of His-tagged huCD4 with increasing amounts (400 and 800 mU of
452 RT) of indicated SHIV virions. Immunoblotting performed using anti-HIV-1 gp120 and anti-6x-His
453 antibodies.

454

455 **Acknowledgments**

456 We thank Julie Overbaugh for supporting the development of $rhCD4_{LOW}$ and $rhCD4_{HIGH}$ cells lines
457 described here (NIDA DP1 DA039543), Ronald Desrosiers for providing the immortalized 221 T-
458 lymphocytes, and Kyle Yamat for technical assistance. The following reagents were obtained
459 through the NIH HIV Reagent Program, Division of AIDS, NIAID, NIH: TZM-bl cells (contributed
460 by John Kappes and Xiaoyun Wu), Cf2Th/syn CCR5 cells (contributed by Tajib Mirzabekov and
461 Joseph Sodroski), and HIV-1 gp120 antiserum (contributed by Michael Phelan).

462 **Funding**

463 This work was supported by grants from the National Institutes of Health (NIAID R00 AI125136
464 to AS and NIDA 1DP2DA049279-01 to AH) and The Ohio State University's institutional start-up
465 funds to AS.

466 **Author contributions**

467 Conceptualization: AS; research design: AH, AS; investigation: GVV, ACS, HCB, AS; contributed
468 methods/reagents: RKS, RCL; writing—original draft: AS; writing—review and editing: all authors.

469

470 **References**

471 1. Hatziioannou T, Evans DT. 2012. Animal models for HIV/AIDS research. Nat Rev
472 Microbiol 10:852-67.
473 2. Sharma A, Boyd DF, Overbaugh J. 2015. Development of SHIVs with circulating,
474 transmitted HIV-1 variants. J Med Primatol 44:296-300.
475 3. Chen Z, Huang Y, Zhao X, Skulsky E, Lin D, Ip J, Gettie A, Ho DD. 2000. Enhanced
476 infectivity of an R5-tropic simian/human immunodeficiency virus carrying human
477 immunodeficiency virus type 1 subtype C envelope after serial passages in pig-tailed
478 macaques (Macaca nemestrina). J Virol 74:6501-10.
479 4. Harouse JM, Gettie A, Eshetu T, Tan RC, Bohm R, Blanchard J, Baskin G, Cheng-Mayer
480 C. 2001. Mucosal transmission and induction of simian AIDS by CCR5-specific
481 simian/human immunodeficiency virus SHIV(SF162P3). J Virol 75:1990-5.
482 5. Ndung'u T, Lu Y, Renjifo B, Touzjian N, Kushner N, Pena-Cruz V, Novitsky VA, Lee TH,
483 Essex M. 2001. Infectious simian/human immunodeficiency virus with human
484 immunodeficiency virus type 1 subtype C from an African isolate: rhesus macaque model.
485 J Virol 75:11417-25.
486 6. Nishimura Y, Shingai M, Willey R, Sadjadpour R, Lee WR, Brown CR, Brenchley JM,
487 Buckler-White A, Petros R, Eckhaus M, Hoffman V, Igarashi T, Martin MA. 2010.
488 Generation of the pathogenic R5-tropic simian/human immunodeficiency virus SHIVAD8
489 by serial passaging in rhesus macaques. J Virol 84:4769-81.
490 7. Pal R, Taylor B, Foulke JS, Woodward R, Merges M, Praschunus R, Gibson A, Reitz M.
491 2003. Characterization of a simian human immunodeficiency virus encoding the envelope
492 gene from the CCR5-tropic HIV-1 Ba-L. J Acquir Immune Defic Syndr 33:300-7.
493 8. Song RJ, Chenine AL, Rasmussen RA, Ruprecht CR, Mirshahidi S, Grisson RD, Xu W,
494 Whitney JB, Goins LM, Ong H, Li PL, Shai-Kobiler E, Wang T, McCann CM, Zhang H,

495 Wood C, Kankasa C, Secor WE, McClure HM, Strobert E, Else JG, Ruprecht RM. 2006.
496 Molecularly cloned SHIV-1157ipd3N4: a highly replication- competent, mucosally
497 transmissible R5 simian-human immunodeficiency virus encoding HIV clade C Env. J Virol
498 80:8729-38.
499 9. Sharma A, Overbaugh J. 2018. CD4-HIV-1 Envelope Interactions: Critical Insights for the
500 Simian/HIV/Macaque Model. AIDS Res Hum Retroviruses 34:778-779.
501 10. Boyd DF, Peterson D, Haggarty BS, Jordan AP, Hogan MJ, Goo L, Hoxie JA, Overbaugh
502 J. 2015. Mutations in HIV-1 envelope that enhance entry with the macaque CD4 receptor
503 alter antibody recognition by disrupting quaternary interactions within the trimer. J Virol
504 89:894-907.
505 11. Munro JB, Gorman J, Ma X, Zhou Z, Arthos J, Burton DR, Koff WC, Courter JR, Smith
506 AB, 3rd, Kwong PD, Blanchard SC, Mothes W. 2014. Conformational dynamics of single
507 HIV-1 envelope trimers on the surface of native virions. Science 346:759-63.
508 12. Ma X, Lu M, Gorman J, Terry DS, Hong X, Zhou Z, Zhao H, Altman RB, Arthos J,
509 Blanchard SC, Kwong PD, Munro JB, Mothes W. 2018. HIV-1 Env trimer opens through
510 an asymmetric intermediate in which individual protomers adopt distinct conformations.
511 Elife 7.
512 13. Wang Q, Finzi A, Sodroski J. 2020. The Conformational States of the HIV-1 Envelope
513 Glycoproteins. Trends Microbiol 28:655-667.
514 14. Kwon YD, Finzi A, Wu X, Dogo-Isonagie C, Lee LK, Moore LR, Schmidt SD, Stuckey J,
515 Yang Y, Zhou T, Zhu J, Vicic DA, Debnath AK, Shapiro L, Bewley CA, Mascola JR,
516 Sodroski JG, Kwong PD. 2012. Unliganded HIV-1 gp120 core structures assume the CD4-
517 bound conformation with regulation by quaternary interactions and variable loops. Proc
518 Natl Acad Sci U S A 109:5663-8.
519 15. Herschhorn A, Gu C, Moraca F, Ma X, Farrell M, Smith AB, 3rd, Pancera M, Kwong PD,
520 Schon A, Freire E, Abrams C, Blanchard SC, Mothes W, Sodroski JG. 2017. The beta20-

521 beta21 of gp120 is a regulatory switch for HIV-1 Env conformational transitions. Nat
522 Commun 8:1049.
523 16. Herschhorn A, Ma X, Gu C, Ventura JD, Castillo-Menendez L, Melillo B, Terry DS, Smith
524 AB, 3rd, Blanchard SC, Munro JB, Mothes W, Finzi A, Sodroski J. 2016. Release of gp120
525 Restraints Leads to an Entry-Competent Intermediate State of the HIV-1 Envelope
526 Glycoproteins. mBio 7.
527 17. Humes D, Emery S, Laws E, Overbaugh J. 2012. A species-specific amino acid difference
528 in the macaque CD4 receptor restricts replication by global circulating HIV-1 variants
529 representing viruses from recent infection. J Virol 86:12472-83.
530 18. Keele BF, Giorgi EE, Salazar-Gonzalez JF, Decker JM, Pham KT, Salazar MG, Sun C,
531 Grayson T, Wang S, Li H, Wei X, Jiang C, Kirchherr JL, Gao F, Anderson JA, Ping LH,
532 Swanstrom R, Tomaras GD, Blattner WA, Goepfert PA, Kilby JM, Saag MS, Delwart EL,
533 Busch MP, Cohen MS, Montefiori DC, Haynes BF, Gaschen B, Athreya GS, Lee HY,
534 Wood N, Seoighe C, Perelson AS, Bhattacharya T, Korber BT, Hahn BH, Shaw GM. 2008.
535 Identification and characterization of transmitted and early founder virus envelopes in
536 primary HIV-1 infection. Proc Natl Acad Sci U S A 105:7552-7.
537 19. Han Q, Jones JA, Nicely NI, Reed RK, Shen X, Mansouri K, Louder M, Trama AM, Alam
538 SM, Edwards RJ, Bonsignori M, Tomaras GD, Korber B, Montefiori DC, Mascola JR,
539 Seaman MS, Haynes BF, Saunders KO. 2019. Difficult-to-neutralize global HIV-1 isolates
540 are neutralized by antibodies targeting open envelope conformations. Nat Commun
541 10:2898.
542 20. Humes D, Overbaugh J. 2011. Adaptation of subtype a human immunodeficiency virus
543 type 1 envelope to pig-tailed macaque cells. J Virol 85:4409-20.
544 21. Alexander L, Du Z, Rosenzweig M, Jung JU, Desrosiers RC. 1997. A role for natural
545 simian immunodeficiency virus and human immunodeficiency virus type 1 nef alleles in
546 lymphocyte activation. J Virol 71:6094-9.

547 22. Finzi A, Xiang SH, Pacheco B, Wang L, Haight J, Kassa A, Danek B, Pancera M, Kwong
548 PD, Sodroski J. 2010. Topological layers in the HIV-1 gp120 inner domain regulate gp41
549 interaction and CD4-triggered conformational transitions. Mol Cell 37:656-67.
550 23. Haim H, Strack B, Kassa A, Madani N, Wang L, Courter JR, Princiotto A, McGee K,
551 Pacheco B, Seaman MS, Smith AB, 3rd, Sodroski J. 2011. Contribution of intrinsic
552 reactivity of the HIV-1 envelope glycoproteins to CD4-independent infection and global
553 inhibitor sensitivity. PLoS Pathog 7:e1002101.
554 24. Kassa A, Madani N, Schon A, Haim H, Finzi A, Xiang SH, Wang L, Princiotto A, Pancera
555 M, Courter J, Smith AB, 3rd, Freire E, Kwong PD, Sodroski J. 2009. Transitions to and
556 from the CD4-bound conformation are modulated by a single-residue change in the human
557 immunodeficiency virus type 1 gp120 inner domain. J Virol 83:8364-78.
558 25. Xiang SH, Kwong PD, Gupta R, Rizzuto CD, Casper DJ, Wyatt R, Wang L, Hendrickson
559 WA, Doyle ML, Sodroski J. 2002. Mutagenic stabilization and/or disruption of a CD4-
560 bound state reveals distinct conformations of the human immunodeficiency virus type 1
561 gp120 envelope glycoprotein. J Virol 76:9888-99.
562 26. Joag SV, Li Z, Foresman L, Stephens EB, Zhao LJ, Adany I, Pinson DM, McClure HM,
563 Narayan O. 1996. Chimeric simian/human immunodeficiency virus that causes
564 progressive loss of CD4+ T cells and AIDS in pig-tailed macaques. J Virol 70:3189-97.
565 27. Tan RC, Harouse JM, Gettie A, Cheng-Mayer C. 1999. In vivo adaptation of SHIV(SF162):
566 chimeric virus expressing a NSI, CCR5-specific envelope protein. J Med Primatol 28:164-
567 8.
568 28. Ren W, Mumbauer A, Gettie A, Seaman MS, Russell-Lodrigue K, Blanchard J,
569 Westmoreland S, Cheng-Mayer C. 2013. Generation of lineage-related, mucosally
570 transmissible subtype C R5 simian-human immunodeficiency viruses capable of AIDS
571 development, induction of neurological disease, and coreceptor switching in rhesus
572 macaques. J Virol 87:6137-49.

573 29. Li H, Wang S, Kong R, Ding W, Lee FH, Parker Z, Kim E, Learn GH, Hahn P, Policicchio
574 B, Brocca-Cofano E, Deleage C, Hao X, Chuang GY, Gorman J, Gardner M, Lewis MG,
575 Hatziioannou T, Santra S, Apetrei C, Pandrea I, Alam SM, Liao HX, Shen X, Tomaras GD,
576 Farzan M, Chertova E, Keele BF, Estes JD, Lifson JD, Doms RW, Montefiori DC, Haynes
577 BF, Sodroski JG, Kwong PD, Hahn BH, Shaw GM. 2016. Envelope residue 375
578 substitutions in simian-human immunodeficiency viruses enhance CD4 binding and
579 replication in rhesus macaques. Proc Natl Acad Sci U S A 113:E3413-22.
580 30. Del Prete GQ, Ailers B, Moldt B, Keele BF, Estes JD, Rodriguez A, Sampias M, Oswald
581 K, Fast R, Trubey CM, Chertova E, Smedley J, LaBranche CC, Montefiori DC, Burton DR,
582 Shaw GM, Markowitz M, Piatak M, Jr., KewalRamani VN, Bieniasz PD, Lifson JD,
583 Hatziioannou T. 2014. Selection of unadapted, pathogenic SHIVs encoding newly
584 transmitted HIV-1 envelope proteins. Cell Host Microbe 16:412-8.
585 31. Chang HW, Tartaglia LJ, Whitney JB, Lim SY, Sanisetty S, Lavine CL, Seaman MS,
586 Rademeyer C, Williamson C, Ellingson-Strouss K, Stamatatos L, Kublin J, Barouch DH.
587 2015. Generation and evaluation of clade C simian-human immunodeficiency virus
588 challenge stocks. J Virol 89:1965-74.
589 32. Wei X, Decker JM, Liu H, Zhang Z, Arani RB, Kilby JM, Saag MS, Wu X, Shaw GM,
590 Kappes JC. 2002. Emergence of resistant human immunodeficiency virus type 1 in
591 patients receiving fusion inhibitor (T-20) monotherapy. Antimicrob Agents Chemother
592 46:1896-905.
593 33. Farzan M, Mirzabekov T, Kolchinsky P, Wyatt R, Cayabyab M, Gerard NP, Gerard C,
594 Sodroski J, Choe H. 1999. Tyrosine sulfation of the amino terminus of CCR5 facilitates
595 HIV-1 entry. Cell 96:667-76.
596 34. Nahabedian J, Sharma A, Kaczmarek ME, Wilkerson GK, Sawyer SL, Overbaugh J. 2017.
597 Owl monkey CCR5 reveals synergism between CD4 and CCR5 in HIV-1 entry. Virology
598 512:180-186.

599 35. Sharma A, McLaughlin RN, Jr., Basom RS, Kikawa C, OhAinle M, Yount JS, Emerman M,
600 Overbaugh J. 2019. Macaque interferon-induced transmembrane proteins limit replication
601 of SHIV strains in an Envelope-dependent manner. PLoS Pathog 15:e1007925.
602 36. Meyerson NR, Sharma A, Wilkerson GK, Overbaugh J, Sawyer SL. 2015. Identification of
603 Owl Monkey CD4 Receptors Broadly Compatible with Early-Stage HIV-1 Isolates. J Virol
604 89:8611-22.
605 37. Wu X, Parast AB, Richardson BA, Nduati R, John-Stewart G, Mbori-Ngacha D, Rainwater
606 SM, Overbaugh J. 2006. Neutralization escape variants of human immunodeficiency virus
607 type 1 are transmitted from mother to infant. J Virol 80:835-44.
608 38. Boyd DF, Sharma A, Humes D, Cheng-Mayer C, Overbaugh J. 2016. Adapting SHIVs In
609 Vivo Selects for Envelope-Mediated Interferon-alpha Resistance. PLoS Pathog
610 12:e1005727.
611 39. Cavrois M, De Noronha C, Greene WC. 2002. A sensitive and specific enzyme-based
612 assay detecting HIV-1 virion fusion in primary T lymphocytes. Nat Biotechnol 20:1151-4.
613 40. Roesch F, OhAinle M, Emerman M. 2018. A CRISPR screen for factors regulating
614 SAMHD1 degradation identifies IFITMs as potent inhibitors of lentiviral particle delivery.
615 Retrovirology 15:26.
616 41. Selig L, Pages JC, Tanchou V, Preveral S, Berlioz-Torrent C, Liu LX, Erdtmann L, Darlix
617 J, Benarous R, Benichou S. 1999. Interaction with the p6 domain of the gag precursor
618 mediates incorporation into virions of Vpr and Vpx proteins from primate lentiviruses. J
619 Virol 73:592-600.
620 42. Vermeire J, Naessens E, Vanderstraeten H, Landi A, Iannucci V, Van Nuffel A, Taghon T,
621 Pizzato M, Verhasselt B. 2012. Quantification of reverse transcriptase activity by real-time
622 PCR as a fast and accurate method for titration of HIV, lenti- and retroviral vectors. PLoS
623 One 7:e50859.

624 **Figure 1**

625

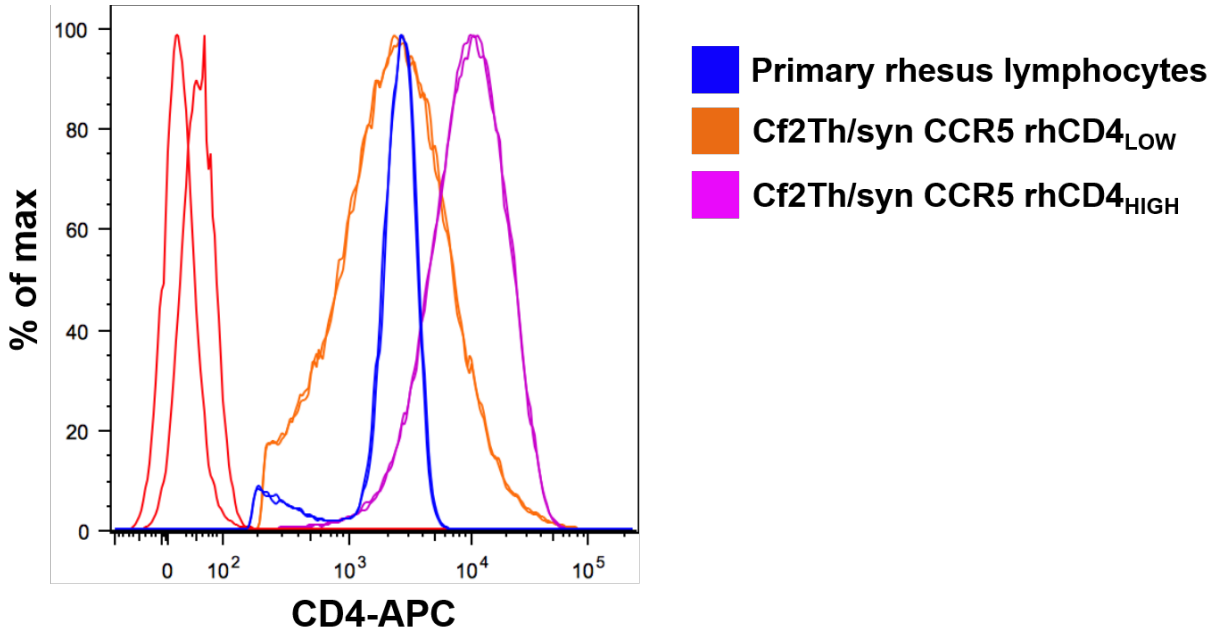

626

627

628

629

630

631

632

633

634

635

636

637

638

639

640

641

642

643 **Figure 2**

644

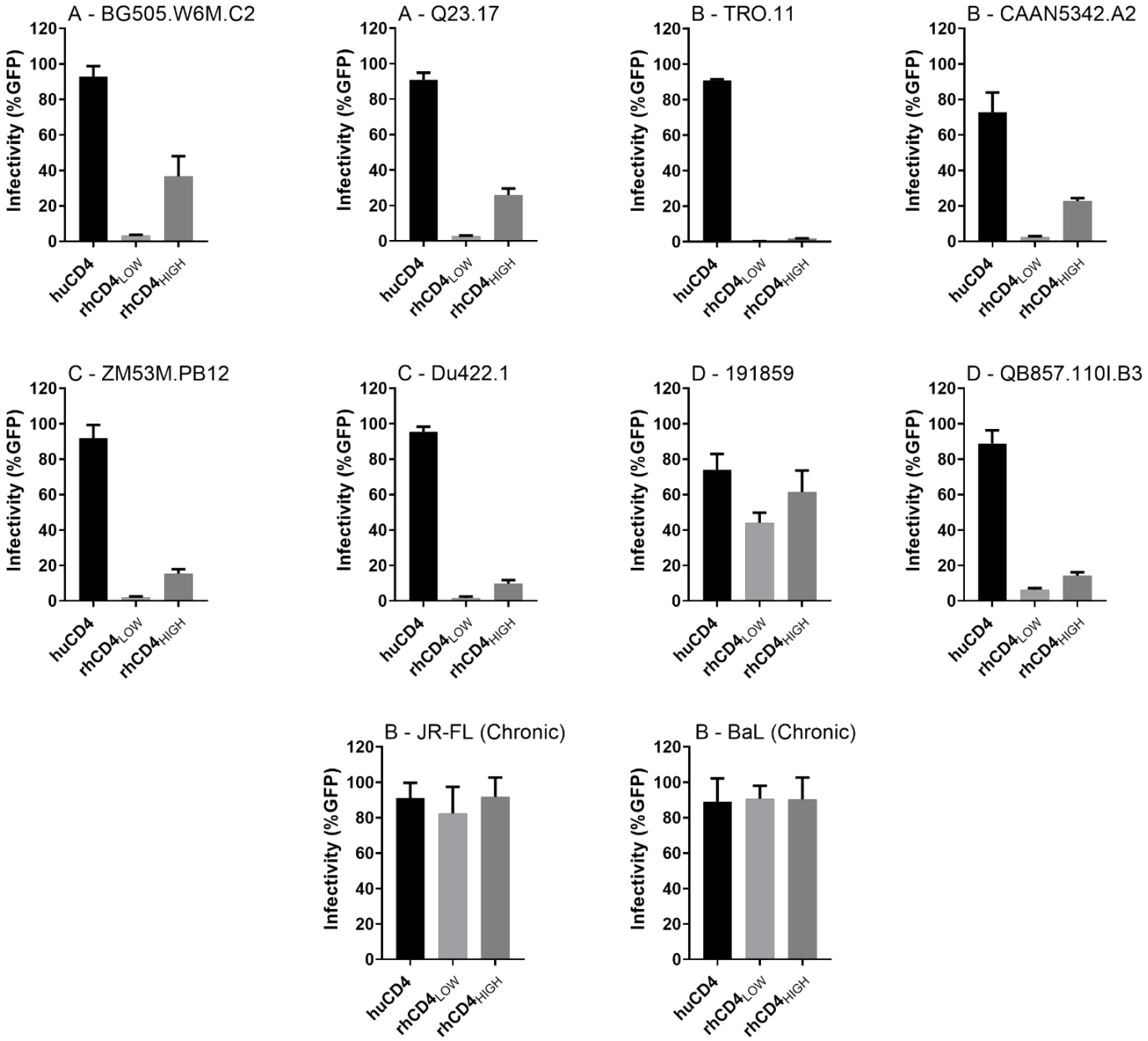

645

646

647

648

649

650

651 **Figure 3**

652

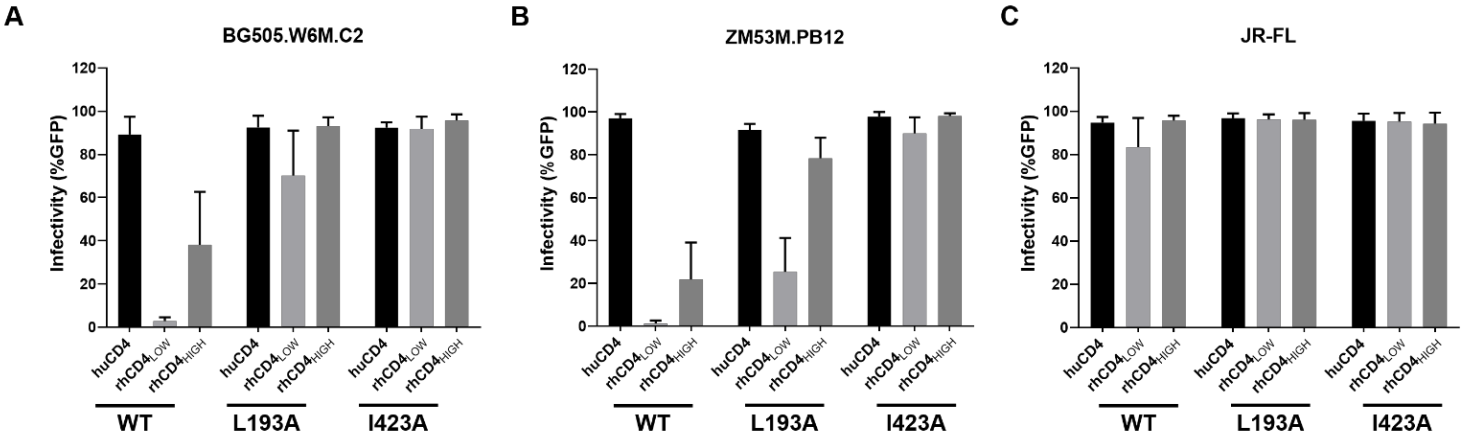

653

654

655

656

657

658

659

660

661

662

663

664

665

666

667

668

669

670

671

672

673 **Figure 4**

674

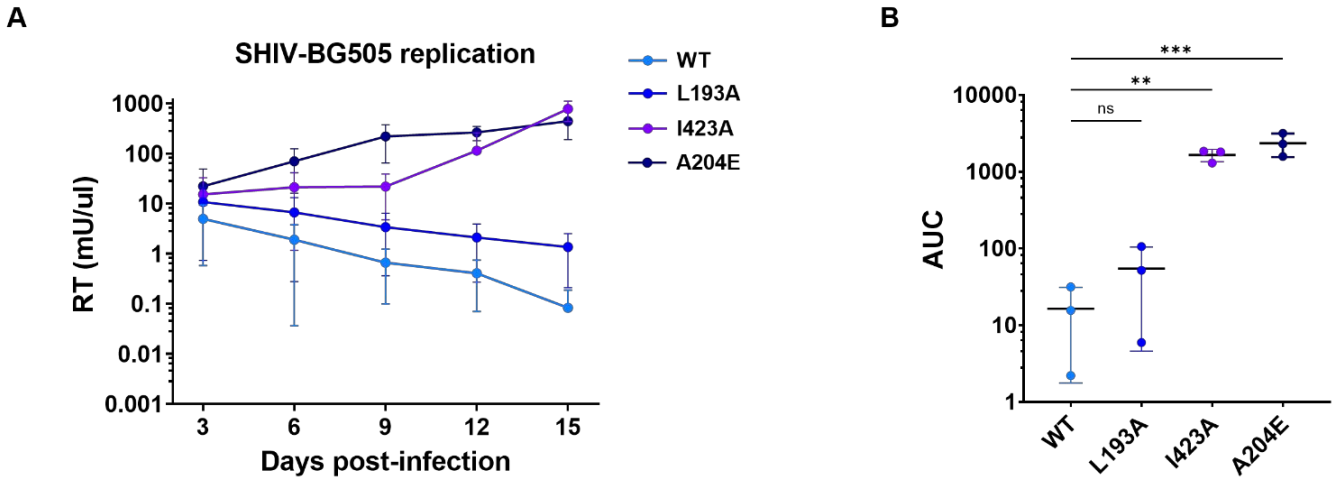

675

676

677

678

679

680

681

682

683

684

685

686

687

688

689

690

691

692

693

694 **Figure 5**

695

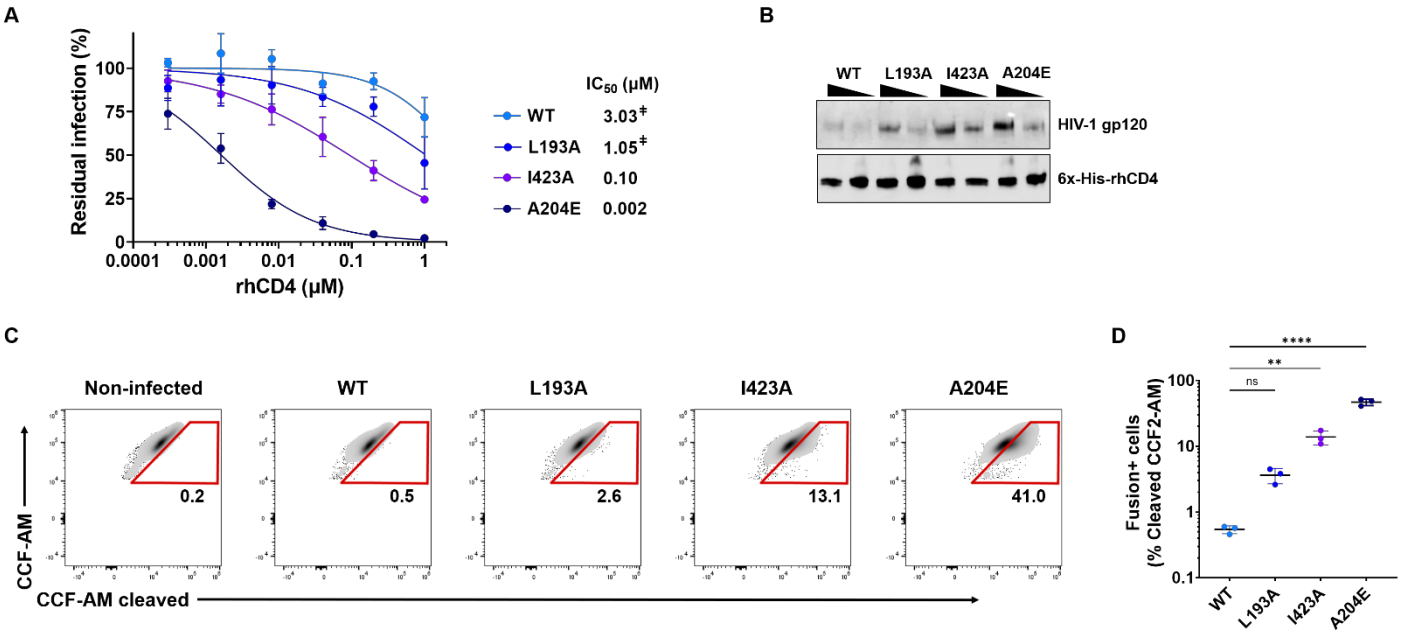

696

697

698

699

700

701

702

703

704

705

706

707

708

709

710

711

712

713 **Figure S1**

714

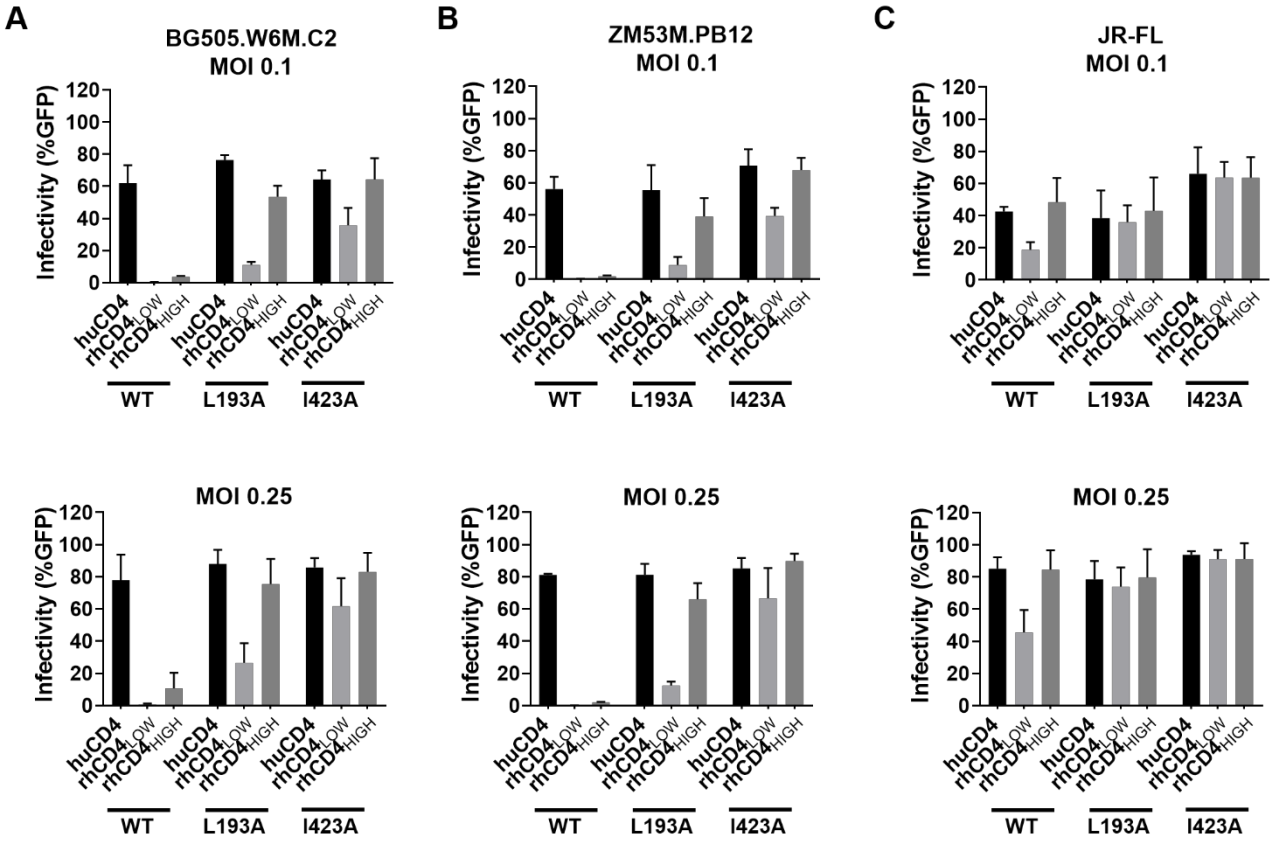

715

716

717

718

719

720

721

722

723

724

725

726

727

728

729 **Figure S2**

730

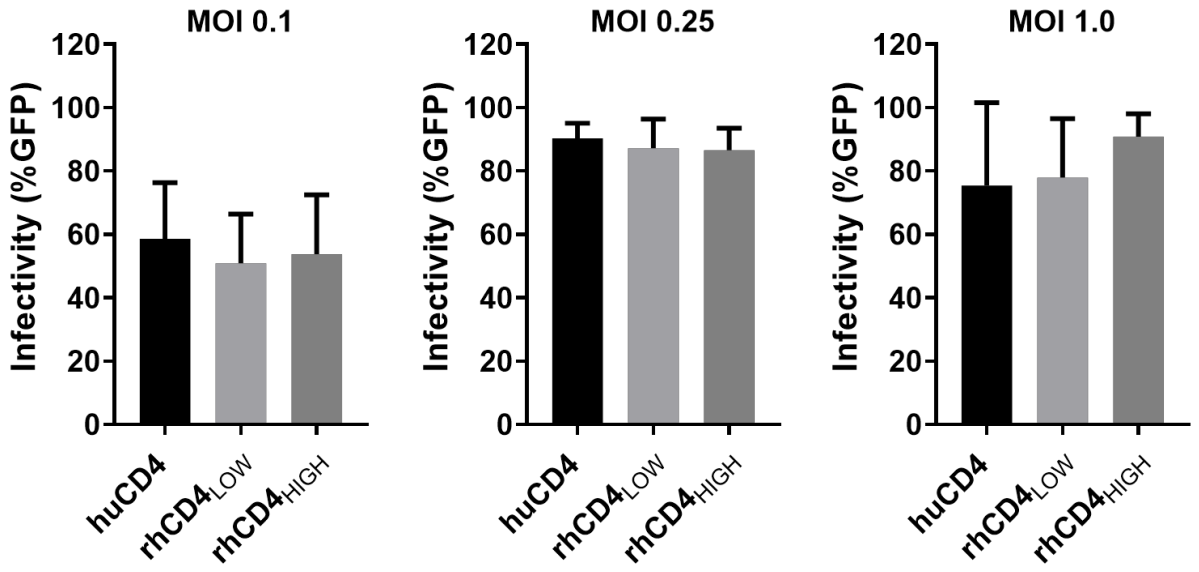

731

732

733

734

735

736

737

738

739

740

741

742

743

744

745

746

747

748

749 **Figure S3**

750

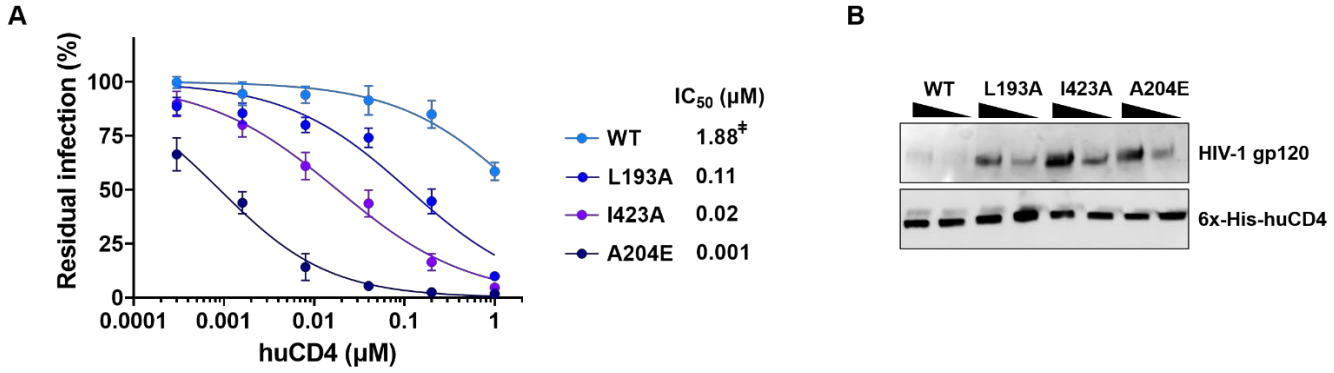

751

752

753

754

755

756

757

758

759

760

761

762

763

764

765

766

767

768

769

770

771

772

773 **Table 1: Transmitted/founder and early-stage Env clones used in this study.**
774

Envelope clone	Subtype	Mode of transmission[a]	Source[b]	GenBank accession no.	Time post infection (weeks)
BG505.W6M.C2	A	M-C	PBMC	DQ208458	6
Q23.17	A	M-F	PBMC	AF004885	11
TRO.11	B	M-M	ccPBMC	AY835445	4
CAAN5342.A2	B	M-M	Plasma	AY835452	<12
Du422.1	C	M-F	ccPBMC	DQ411854	8
ZM53M.PB12	C	F-M	PBMC	AY423984	<12
QB857.110I.B3	D	M-F	PBMC	FJ866138	16
191859	D	M-F	Plasma	JX203064	Fiebig I

775
776
777 [a] M-C: Mother to Child; M-F: Male to Female; M-M: Male to Male; F-M: Female to Male.
778 [b] PBMC: Env cloned from uncultured PBMCs isolated directly from patient; ccPBMC: Patient
779 PBMCs (or virus from these PBMCs) underwent short-term coculture with PBMCs from HIV-1-
780 negative donors to amplify virus before cloning; Plasma: Env cloned from virion RNA in plasma
781 isolated directly from patient.
782